Excited-State Dynamics and Self-Organization of Poly(3-hexylthiophene) (P3HT) in Solution and Thin Films

Bruno Ferreira,[1] Palmira Ferreira da Silva,*,[1] J. Sérgio Seixas de Melo,[2] João Pina,[2] and António Maçanita*,[1]

[1]Centro de Química Estrutural, Instituto Superior Técnico, Technical University of Lisbon, Avenida Rovisco Pais s/n, 1049-001 Lisbon, Portugal

[2]Department of Chemistry, University of Coimbra, Rua Larga, 3004-535 Coimbra, Portugal

ABSTRACT: The fluorescence decays of a stereoregular head-to-tail RR-HT poly(3-hexylthiophene), P3HT, in methylcyclohexane (MCH) are described by sums of three or four exponential terms, respectively above and below −10 °C. In the high-temperature region, the polymer lifetime (ca. 500 ps) is accompanied by two shorter decay times (ca. 20 and 120 ps), which are assigned to intrachain energy transfer from high to lower energy excitons on the basis of temperature and wavelength dependence of the fluorescence decays. The absence of conformational (torsional) relaxation is attributed to the small dihedral angle between monomers that is predicted for the stereoregular polymer in the ground state. Below −10 °C, the polymer forms excimer-like aggregates, showing vibrational structured absorption and emission bands similar to those observed in thin films. The vibrational structure is attributed to a deep minimum in the ground-state energy surface of the dimer or aggregate. Below −40 °C, the fluorescence measured at the aggregate emission wavelength (670 nm) basically results from direct excitation of the aggregate and decays with a sum of three exponential terms (decay times of ca. 0.14, 0.6, and 1.5 ns, with similar weights).

Because the spectral similarities between film and aggregates indicate similar electronic first singlet excited states (and oscillator strengths), the much shorter decay times (0.05, 0.15, and 0.43 ns) and lower fluorescence quantum yield of P3HT in films are assigned to efficient exciton dissociation and/or phonon-induced internal conversion competing with radiative decay (>1 ns).
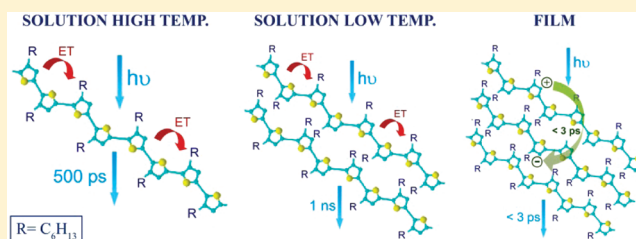
INTRODUCTION

Decay mechanisms in organic conjugated polymers and oligomers have gained an increased interest in the past years. This happens because the detailed understanding of the complex processes occurring in π-conjugated polymers is relevant in the tuning of the photophysical processes occurring in these systems, which has led to the development of new functional polymeric materials for optoelectronic applications.[1] Among other factors, the performance of devices based on π-conjugated polymers is strongly dependent upon the transport of excitation along and across the polymer chains. Therefore, it is of utmost relevance to understand the way the flow of excitation energy in conjugated polymers happens and the various factors that can influence this transfer.

Energy migration processes in polymer/fullerene blends have also been widely investigated for solar energy conversion applications.[2−6] The classical example, which has been intensively exploited and has shown potential successful applications in solar cell devices, involves the donor−acceptor system made of poly(3-hexylthiophene) (P3HT) and the fullerene derivative [6,6]-phenyl-C_{61}-butyric acid methyl ester (PCBM).[7]

Upon photoexcitation, the fast decay components observed in conjugated polymers are attributed to intrachain excitation energy transfer along the π-conjugated system and/or to a conformational (torsional) relaxation process (from an instantaneously generated to a more relaxed structure) which in both cases lead to an emission from a lower energy state, conformer or structure.[8−16]

Among the numerous studies on this P3HT/PCBM system, some are relevant to the understanding of the present work, particularly those which have dealt with the dynamics of the decay processes in solution or solid state. Xie et al.[17] reported a femtosecond-time-resolved fluorescence study of a regioregular P3HT (RR-P3HT) in solution and in blend films made of P3HT/PCBM. Excitation energy transfer, between segments, and torsional relaxation were found to be competitive processes occurring in a time scale of several picoseconds. Rising components were observed in the decays collected at the low-energy part of the emission band, suggesting that these were leading to the formation of relatively lower energy emission states (at 650 and 700 nm). In the film, excitonic quenching (charge transfer) was found as the dominant process (found in the femtosecond time scale), whereas excitation energy transfer was found to occur in the picosecond time domain (7−11 ps). In thermally annealed blend films, due to
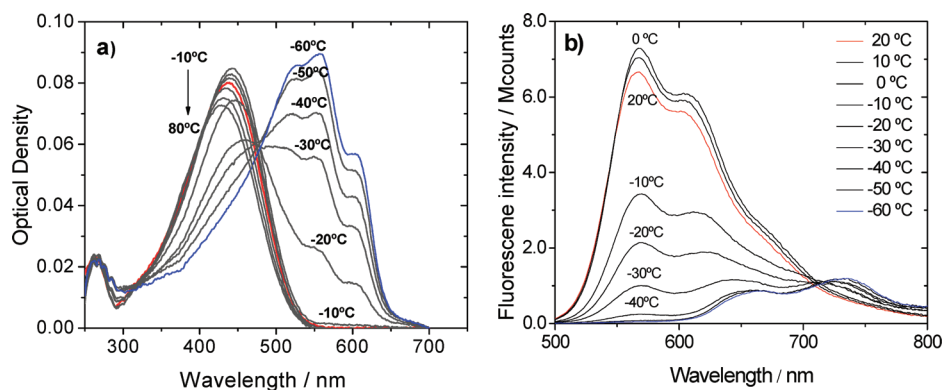
Figure 1. Absorption and emission spectra of P3HT in methylcyclohexane (3.8×10^{-8} mol/L), as a function of temperature: (a) absorption spectra and (b) fluorescence spectra (λ_{exc} = 440 nm).

more organized nanodomains formed, the charge transfer (334 fs) and downhill relaxation (942 fs) of dynamic localized (self-trapped) excitons were found to be competitive processes. Still in films energy migration along or between P3HT chains was also observed in a time scale of ~100 ps.

Herz et al.[18] have proposed that with P3HT aggregates (in films) torsional relaxation occurs in ~13 ps, a value presumably in agreement with that of others.[19] Others have found for a 90% regio-regular P3HT in clorobenzene solution a 600 ps decay component (attributed to the deactivation of the S_1 state) and a 300 ns decay for the triplet, whereas in film two species were present (in the picosecond to nanosecond time range): the singlet excited state (decaying with ~400 ps) and the polaron state (decaying with a bimolecular rate of 5×10^{-11} cm^3 s^{-1}).[20]

Exciton diffusion in films of varying thickness (6.5−32 nm) have also been investigated in silica and TiO$_2$ supports, and it was found that, independently of the film thickness, the titanium oxide support leads to a faster decay (higher quenching effect) than in silica. In the case of the thinnest film (6.5 nm) the value was reported to be of 250 ps.[21]

More recently, also in chlorobenzene and thin films, Heeger and co-workers have performed a detailed investigation of regioregular P3HT with femtosecond-up-conversion (200 fs resolution) and found tetraexponential decays with decay time values of ca. 0.5, 5.0, 50, and 500 ps, slightly depending on the experimental conditions (film or solution and excitation wavelength).[22] They have concluded that, in both film and solution, the initially highly delocalized and mobile electrons and holes self-localize within ~100 fs and that this relaxation process involves C=C stretching and a torsional vibrational mode.[22] However, this view may be confronted with the general wisdom in conjugated polymers that tightly bound excitons (Frenkel excitons) are formed instantaneously with excitation.

In blend films of P3HT:PCBM it was reported, again based on femtosecond-fluorescence up-conversion data, that the polymer exciton relaxation phenomena, which in this case include diffusion-controlled exciton−exciton annihilation and electron transfer, occurs on a 100 fs time scale, that is, even before diffusive exciton migration may take place.[3]

In this work we have made a complete analysis of the photophysics of P3HT in solution, in thin films, and in time scales varying from few hundreds of femtoseconds to picosecond and nanosecond time scales. It is shown, on the basis of the dependence on temperature, that the short

component(s) in the decay profiles are independent of temperature and therefore barrierless, which goes in line with the view that the deactivation process in P3HT is mainly due to energy migration (exciton diffusion) along conjugated segments of the polymer backbone. This is in agreement with other previous findings with polythiophene derivatives where exciton energy migration has been found to be responsible for the initial (and fast) decay components.[10,11]

■ EXPERIMENTAL SECTION

Samples. Poly(3-hexythiophene) (M_w = 87 kD, 89% regioregular) was purchased from Aldrich (ref 445703), and purified by column chromatography (SiO$_2$) using CHCl$_3$ as eluent. Tri(3-hexylthiophene) (T3HT) was a kind gift of A. T. Marques and Prof. Ulli Scherf. Spectroscopic purity grade methylcyclohexane, MCH (Fluka), was used without further purification.

Solutions of P3HT in MCH were stirred overnight and then diluted to a final optical density of ca. 0.15 in 10 mm optical length cells, i.e., to a final concentration of thiophene monomers equal to 2×10^{-5} mol/L, or 3.8×10^{-8} mol/L P3HT (87 kD).

Thin films were prepared under N$_2$ atmosphere (glovebox) by spin-coating a 10 mg/mL solution of P3HT in toluene (Riedel-de Haën, Spectranal, 99.9%) on 450 mm^2 quartz disks (UQG Optics) at 1800 rpm, yielding optical densities of ca. 0.25. For femtosecond measurements, the solution was spin-coated on 11 cm^2 rotating quartz disks of the FOG-100 (see below). In both cases the films were protected with a second disk and kept in the glovebox until measurement.

Methods. UV−vis absorption spectra were recorded on a Beckman DU-70 spectrophotometer. Fluorescence emission and excitation spectra were measured using a SPEX Fluorolog 212I spectrofluorimeter, in the S/R mode, and corrected for optics and detector wavelength dependence.

Fluorescence decays were measured using the time-correlated single-photon counting (TCSPC) and fluorescence up-conversion (FUC) techniques. The TCSPC equipment was previously described:[23] the excitation was provided by a Millennia Xs/Tsunami lasers system from Spectra Physics, operating at 82 MHz, and frequency-doubled. The sample emission was collected at the magic angle (Glan-Thompson polarizer), passed through a monochromator (Jobin-Yvon H20 Vis) and detected with a microchannel plate photomultiplier (Hamamatsu R3809u-50). The full width at half-maximum (fwhm) of the instrumental response is 17−18 ps with 814 fs/

channel resolution. For FUC measurements a Millennia Xs laser was used to pump a CDP Systems Inc. setup composed of a femtosecond Ti:saphire laser (TISSA-100), a CDP 2015 frequency doubler/tripler, and a FOG-100 fs optically gated fluorescence kinetic measurement system. The polarization of the (pump) excitation pulses (ca. 200 fs fwhm) was set at the magic angle with respect to the gate pulse. The sample was placed in a rotating cell constituted by two 37.5 mm diameter quartz disks at 1 mm distance). The fluorescence of the sample and the gate beam were overlapped on a nonlinear crystal and the up-converted photons were passed through a CDP2022D double monochromator and detected with a photon counting photomultiplier tube (PMT). All fluorescence decays were deconvoluted from the excitation pulse using the Sand program.[24]

RESULTS

Absorption and Fluorescence Spectra. Absorption and fluorescence spectra of P3HT in MCH, as a function of temperature (−60 to +80 °C) are shown in Figure 1. At 20 °C the absorption spectrum (Figure 1a) shows the broad absorption band of P3HT in the 340−540 nm spectral range with maximum at 440 nm, which shifts to shorter wavelengths (10 nm) upon increasing temperature up to 80 °C, as expected from the temperature induced decrease in the solvent refractive index.

On lowering temperature, this broad absorption band is gradually replaced with a red-shifted well-structured band (three first vibronic transitions at 620, 551, and 520 nm). The low-temperature band starts to appear below temperature values within the −10 to −20 °C temperature range, depending on polymer concentration (the highest the polymer concentration, the highest the starting temperature). The concentration dependence indicates the presence of bimolecular processes, such as dimerization/aggregation, in the origin of the new band. However, an isosbestic wavelength is apparent at 475 nm.

The structured band closely resembles the one previously observed for P3HT in chloroform−alcohol mixtures with high mole fractions of methanol (poor solvent) at room temperature, which has also been assigned to polymer aggregates.[6,25,26]

Fluorescence spectra resulting from excitation at the isosbestic wavelength, 475 nm (Figure 1b), show the expected progressive loss of the first two vibronic peaks at 570 and 605 nm and the appearance of a new emission band with vibronic transitions at 650 and 736 nm, upon lowering temperature. An isoemissive wavelength seems to exist at 713 nm. The-low temperature fluorescence excitation spectra collected at 736 nm (not shown) match the new absorption band.

Contrary to that found in the absorption, the room-temperature fluorescence emission spectra for P3HT display the structured emission band characteristic of these (and related) polymers, thus showing that different potential energy curves (and consequently geometries) are present in the ground and first singlet excited states.[26,27] A similar behavior was found for poly[3-(2,5-dioctylphenyl)thiophene] in toluene solution which was attributed to torsional relaxation (from the excited to the ground state) of conjugated segments leading to a dynamical Stokes shift. Thus, it was proposed that in the ground state the chains are torsionally disordered (due to the shallow torsional potential with a nonplanar equilibrium position), and after vertical excitation the steep profile of the potential energy surface (in the excited state) leads to a

torsional relaxation into more planar conformations (with a quinoid-like character).[28]

The absorption and emission spectra of P3HT films[21,25,29] closely resemble the low-temperature absorption and emission bands, respectively, as noted before[6,26] (Figure 2). However,
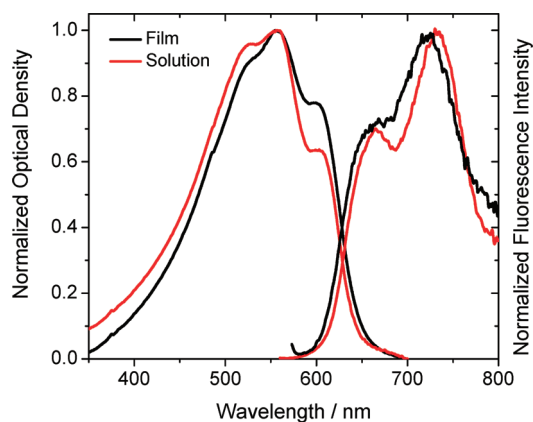
Figure 2. Comparison of absorption and fluorescence emission spectra of P3HT aggregates in MCH solution at −80 °C (red) and P3HT in spin-coated films (black).

the fluorescence intensity is visibly much smaller in the film than in solution in agreement with the small fluorescence quantum yield previously reported for RR-P3HT in films.[20]

Fluorescence Decays of P3HT in MCH as Function of Temperature. Fluorescence decays of P3HT in MCH were measured as a function of temperature with excitation at 434 nm and emission at 540 and 670 nm, which correspond to the onset and the tail of the normal emission band, respectively. Sums of three and four exponential terms were required to properly fit the decays, respectively, above and below −10 °C. Figure 3 shows the global analysis of decays at 20 °C with triple-exponential functions, and at −50 °C with tetraexponential functions.
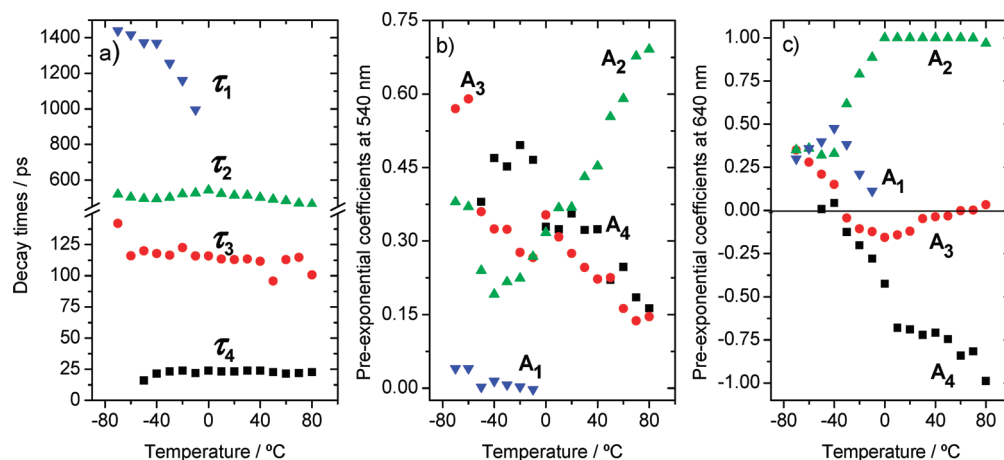
The decay times and preexponential coefficients are plotted against temperature in Figure 4a. The three shortest decay times (τ_4, τ_3, and τ_2, ca. 20, 120, and 500 ps) remain approximately constant within experimental error over the −50 to +80 °C temperature range, while the longest decay time (τ_1), appearing below −10 °C, increases with decreasing temperature from ca. 1 ns at −10 °C to 1.4 ns at −70 °C.

High-Temperature Region. Above −10 °C, the preexponential coefficient of the 500 ps component (A_2), which has been previously assigned to the polymer lifetime,[20,30] is dominant at both wavelengths, and the two shorter decay times appear as decays at 540 nm (positive values of A_3 and A_4 in Figure 4b) and rise times at 670 nm (negative values of A_3 and A_4 in Figure 4c). This means that part of the fluorescence at 670 nm has its origin in some species emitting at 540 nm, a typical signature of energy transfer and/or torsional relaxation in polymers, leading to a time-dependent spectral red shift, resulting from the formation of lower energy excitons.

A more detailed view of this process is shown in Figure 5a, where the preexponential coefficients of the three decay times observed in the fluorescence decays of P3HT measured in MCH at 20 °C ($\tau_4 = 24$ ps, $\tau_3 = 125$ ps, and $\tau_2 = 500$ ps), are plotted as a function of the emission wavelength. The decays at the shortest wavelengths are dominated by the 24 ps decay (A_4), which loses importance (as seen by the decrease in the
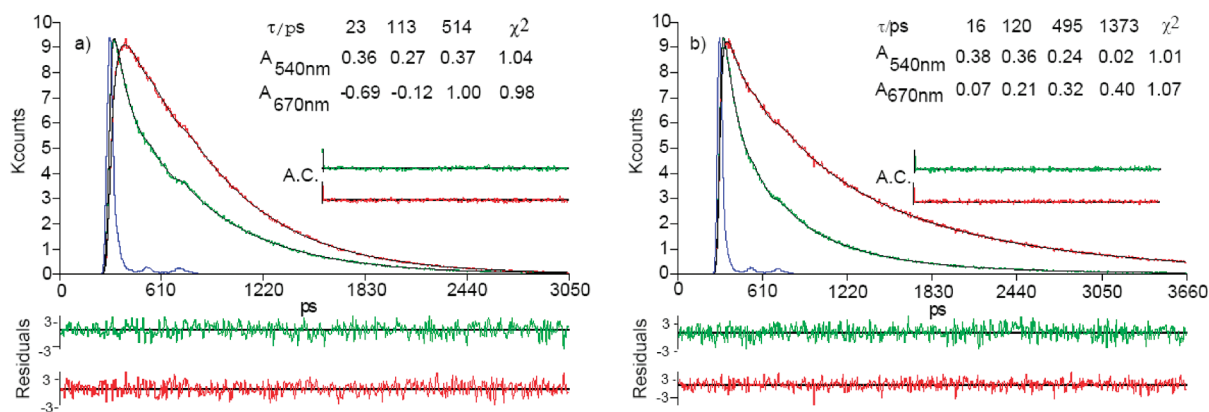
Figure 3. Global fits of the fluorescence decays of P3HT in MCH, measured at two emission wavelengths (540 and 670 nm), with sums of (a) three exponential terms at +20 °C and (b) four exponential terms at −50 °C. The resulting decay times (τ) and preexponential coefficients (A), as well as reduced χ^2 values, weighted residuals, and autocorrelation functions (AC), are shown. The pulse profile, measured with a Ludox solution with optical density matched at the excitation wavelength (λ_{exc}= 434 nm), is shown in blue. The data were collected with 6.1 ps/channel.

Figure 4. Temperature dependence (+80 to −60 °C) of (a) τ and respective A, measured at (b) 540 and (c) 670 nm, of P3HT in MCH. λ_{exc} = 434 nm.
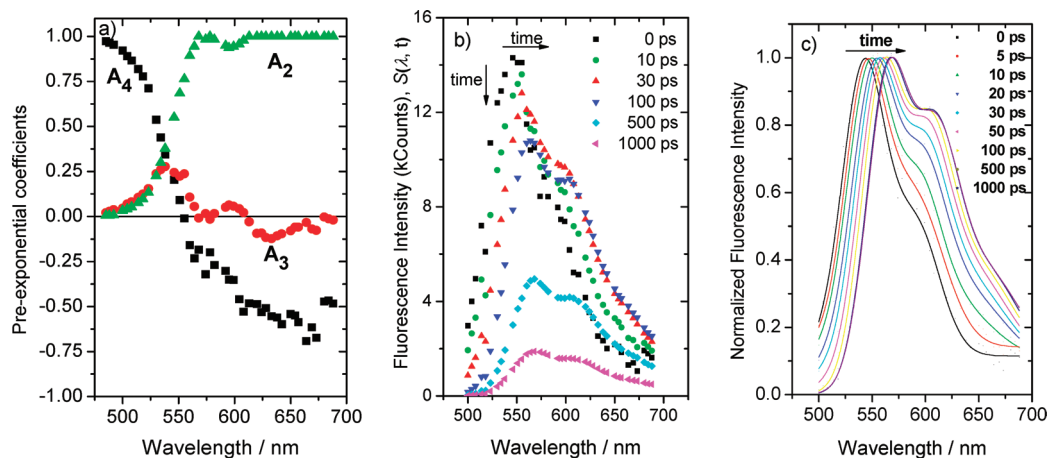

Figure 5. (a) Preexponential coefficients of fluorescence decays of P3HT measured in MCH at 20 °C; (b) time-resolved fluorescence spectra derived from the integrals of the wavelength-resolved decays; (c) time-resolved fluorescence spectra obtained from fitting the data of b with sums of Gaussian functions and normalizing at the 0−0 vibronic transition.

associated preexponential factor) with increasing wavelength up to 555 nm (close to the first vibronic maximum) and becomes a rise-time at above or at the same 555 nm value. The preexponential coefficient of the 125 ps component (A_3) initially increases with increasing the wavelength up to ca. 540

nm, but thereon oscillates, decreasing to negative values above 610 nm.

Emission spectra at different times after excitation $S(\lambda,t)$ were constructed with the fluorescence decays $I(t,\lambda)$, after normalization of their integrals to the steady-state fluorescence
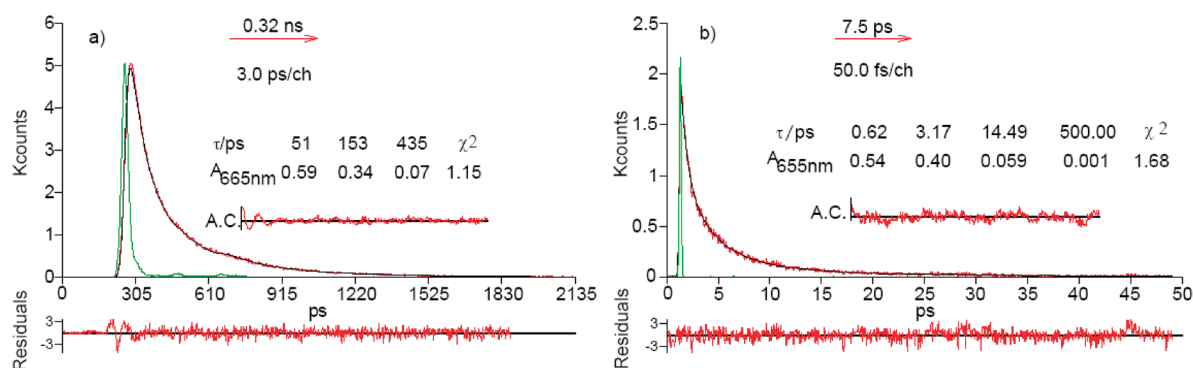
Figure 6. Fluorescence decays of spin-coated films of P3HT measured at 20 °C with (a) ps-TCSPC (3 ps/channel, λ_{ex}= 434 nm, λ_{em}= 655 nm) and (b) fluorescence upconversion (50 fs/step, λ_{ex}= 425 nm, λ_{em}= 655 nm). τ, A, reduced χ^2 values, weighted residuals (WRs) and autocorrelation functions (ACs), are shown. The pulse profile is shown in green.
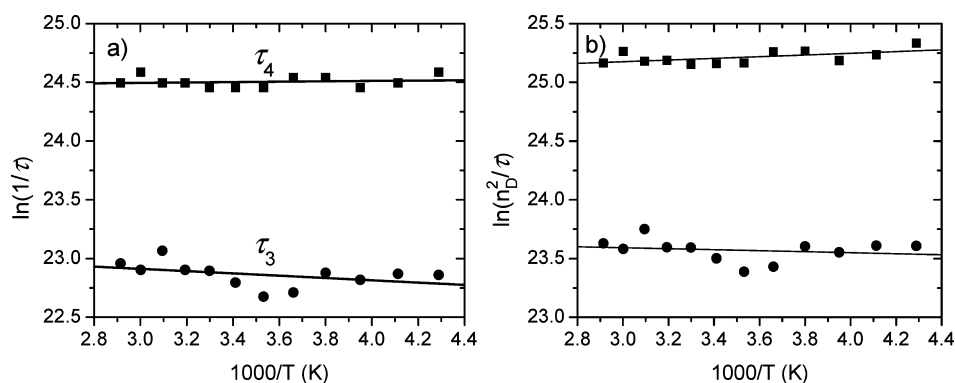
Figure 7. Arrhenius plots of (a) the reciprocals of the two shortest decay times $1/\tau_4$ and $1/\tau_3$ and (b) those of n_D^2/τ_4 and n_D^2/τ_3.

intensity at the respective emission wavelength $S(\lambda,\infty)$ (eq 1). The time-resolved fluorescence spectra (Figure 5b,c) show the above-mentioned red shift (ca. 15 nm in the first 50 ps, plus 8 nm up to 500 ps).

$$S(\lambda, t) = I(t, \lambda)\frac{S_0(\lambda, \infty)}{\int_0^{\infty} I(t, \lambda)\, dt} \quad (1)$$

Low-Temperature Region. Below −10 °C, the decays show an additional longer decay time τ_1, which increases from ca. 1 ns, at −10 °C, to 1.4 ns, at the lowest temperatures. The contribution of τ_1 to the total fluorescence increases at the expenses of that of τ_2 (Figure 4c), being negligible at 540 nm (Figure 4b). It is, thus, assigned to the fluorescence decay of the low-temperature species (aggregates). Below −50 °C the shortest, τ_4 = 20 ps, decay time is not detected (triple-exponential decays).

Fluorescence Decays of P3HT in Films. Figure 6 shows the fluorescence decays of a P3HT film measured at 665 nm with ps-TCSPC (3 ps/channel, λ_{ex} = 434 nm) and fs-FUC (50 fs/delay steps, λ_{ex} = 397 nm).

The ps-TCSPC decay (Figure 6a) shows essentially three exponential terms with short decay times (50, 150, and 430 ps), being the two longer decay times close to, but different from, those observed in MCH solution at −70 °C (see also Discussion). Three unexpected features of this and other decays of P3HT films are as follows: First, the long (nanosecond time range) decay time τ_1 observed for the spectrally similar low-temperature species in MCH is absent. Second, the initial part of the decay cannot be correctly fitted (note the deviations in the weighted residuals and autocorre-

lation plots), and a tetraexponential fit does not remove the problem. Third, the preexponential coefficient of the longest (ca. 500 ps) component strongly depends on the age of the film, decreasing from ~0.5, for measurements made within hours after preparation, to ~0.1 for a 2 month delay between preparation and measurement (the case of Figure 6a). However, in all cases the films were kept in the dark and under N_2 atmosphere (in glovebox), until the measurement has been carried out. These observations have been made with a large number of films and experiments carried out under different experimental conditions and with two different ps-TCSPC apparatuses (Lisbon and Coimbra).

The fs-FUC decay (Figure 6b) clearly shows the presence of two major decay components of ca. 0.6 and 3.2 ps, not resolved in the picosecond decays, which likely are responsible for the earliest time misfit of the ps-TCSPC decays. The very small contribution of the longest decay-time (500 ps, fixed in the analysis) component, when compared to that found in the ps-TCSPC decays, seems to essentially result from the detection of the two shortest lived decay components with large preexponential coefficients (not seen in the ps-TCSPC decays), which due to normalization reduce the preexponential coefficient of the 500 ps component.

■ DISCUSSION

High-Temperature Excited-State Dynamics (Energy Transfer vs Torsional Relaxation). Within the high-temperature region (−10 °C < T < +80 °C), the decays show the intrinsic lifetime of the polymer (τ_2, ca. 500 ps), plus two shorter times (τ_3 and τ_4), appearing as decay times at the band onset and as rise times at the band tail (Figure 4). These

Table 1. Fluorescence Decay Times and Preexponential Coefficients of P3HT in Solvents of Different Viscosities at 20 °C

solvent	η (cP)	n_D	τ_4 (ps)	τ_3 (ps)	τ_2 (ps)	$A_{4,540}$	$A_{3,540}$	$A_{2,540}$	$A_{4,670}$	$A_{3,670}$	$A_{2,670}$
n-hexane	0.294	1.375	26	157	529	0.49	0.13	0.38	−0.37	0.05	0.95
MCH	0.67	1.45	24	126	510	0.42	0.17	0.41	−0.26	−0.11	1
toluene	0.59	1.497	18	103	509	0.62	0.17	0.21	−0.42	−0.01	1

two shorter times could a priori result from conformational (torsional) relaxation, isomerization, and/or energy transfer. Because there is an activation energy for the two first processes ($E_a \approx 2$ kcal/mol in MCH), their respective rate constants should be temperature-dependent, while for energy transfer (no activation energy) the rate constant should not significantly depend on temperature. Arrhenius plots of the two reciprocal shorter lifetimes (Figure 7) show that the dynamic processes in the origin of both decay times are temperature-independent, within the experimental error ($E_{a4} = -0.007$ kcal/mol and $E_{a3} = 0.14$ kcal/mol), and are thus assigned to energy transfer. When the implicit temperature dependence of the energy-transfer rate constant on the solvent refractive index (n_D) is removed, in the Arrhenius plots of n_D^2/τ, the activation energies become $E_{a4} = -0.06$ kcal/mol and $E_{a3} = 0.04$ kcal/mol. {The Förster's rate constant, $k^{\text{Förster}} = (\Phi_D/\tau_D)[8.784 \times 10^{-25} I/(n_D^4 R^6)]$, is proportional to the ratio (Φ_D/τ_D) of the fluorescence quantum yield and lifetime of the energy donor, i.e., to the radiative fluorescence rate constant which, in turn, is proportional to the squared solvent refractive index, n_D^2. Thus, $k^{\text{Förster}}$ is approximately proportional to n_D^{-2}.}

Additionally, τ_3 and τ_4 do not show direct proportionality to solvent viscosity as it would be expected for solvent-dependent torsional relaxation (Table 1). Instead, direct proportionality to the solvent refractive index, which is expectable for Förster energy transfer, apparently exists. Therefore, both times are assigned to energy transfer, thus excluding the presence of experimentally detectable conformational relaxation in P3HT.

Torsional relaxation has been shown to be present in other polymers (e.g., PPV[12,31,32] and PF2/6[9]) including polythiophenes.[22,33] The most plausible cause for its absence in head-to-tail regioregular P3HT (HT-RR-P3HT) is the difference in the mean ground-state dihedral angles (θ) between consecutive monomers in these different polymers. Larger dihedral angles are expected for the non-regioregular or di-disubstituted polythiophenes where conformational relaxation has been observed.[28] In these last cases, the decrease in energy resulting from planarization should induce red shifts that are sufficiently large for detection of torsional relaxation.

Intramolecular exciton relaxation and migration dynamics for a series of three P3HT samples of increasing molecular weight (M_W, ranging from an average of 39 monomers to an average of 168 monomers) was investigated in dilute solution by time and energy resolved fluorescence.[27] In agreement with the present work, the decays measured on the high-energy side of the fluorescence maximum, near the maximum, and on the low-energy side are seen with both rising and decaying components. Within the associated experimental error a lifetime of 500 ps was obtained for the different (M_W) P3HT samples investigated, and it was found that this was independent of both emission wavelength and M_W. Moreover, it was reported that, after photoexcitation of the P3HT polymers, rapid relaxation torsional motions occur within the first 100 fs.[27]

Energy Transfer. The analysis of the time-dependent red shift of the spectra in Figure 5 was carried out using the Stokes shift correlation function, $C(t)$ (eq 2),[19,34] where $\nu(t)$, $\nu(0)$,

and $\nu(\infty)$ represent the frequency of the emission maximum intensity at time $t = t$, $t = 0$, and $t = \infty$ (steady state), respectively (Figure 8).

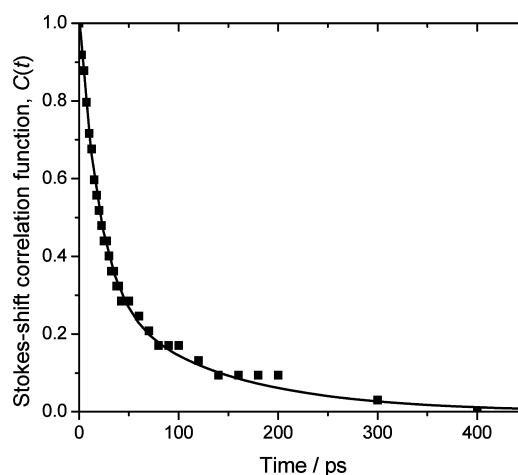$$C(t) = \frac{\nu(t) - \nu(\infty)}{\nu(0) - \nu(\infty)} \tag{2}$$

Figure 8. Stokes shift correlation function $C(t)$ of P3HT in MCH at 20 °C (squares) and respective fit with a sum of two exponential terms (line).

The $C(t)$ function can be fitted with a sum of two exponential terms with decay times of 19.5 ps ($A_2 = 0.69$) and 120 ps ($A_1 = 0.31$). As expected, $C(t)$ is close to the fast part (τ_4 and τ_3) of the TCSPC decays measured at the onset of the emission band (Figure 3) and represents the fluorescence decay of the high-energy excitons (energy donors) in the presence of energy acceptors (lower energy excitons). Because energy transfer leads to nonexponential decays (not given by sums of exponential terms), even in the simplest case of Coulombic (Förster) energy transfer from one donor to an isotropic three-dimensional distribution of energy acceptors,[35] the two shortest decay times and respective preexponential coefficients as a whole represent the energy-transfer process in the time range of the experiment, but each one individually must be regarded as fitting parameters of the much more complex decay expected for energy transfer in polymers.[13] This means that these four parameters (decay times and preexponential coefficients) describe the energy-transfer process within the present experimental time window (6 ps to 3 ns with 6 ps/channel). For different time windows, different parameters are a priori expectable (see below Figure 9).

A final piece of information, in line and in favor of the foregoing considerations/arguments, comes from the comparison of the fluorescence upconversion decays (50 fs/channel) of P3HT (Figure 9) and those of tri(3-hexylthiophene) in MCH at 20 °C, measured at the onset and tail of the emission band. With P3HT additional fast decays (1.2 and 6 ps) are

τ/ps	1.2	6.0	20	500	χ^2
$A_{540\,nm}$	0.28	0.36	0.21	0.15	2.99
$A_{630\,nm}$	-0.26	-0.12	-0.05	1.00	1.73
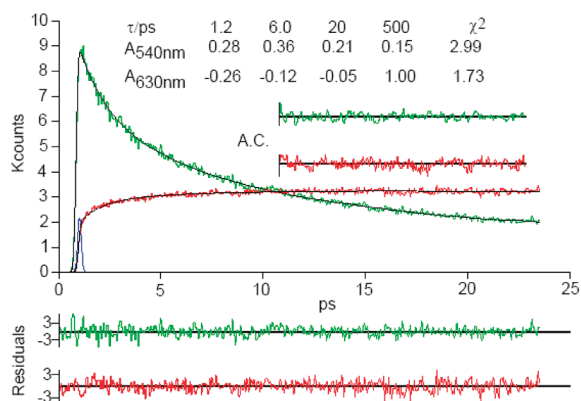
Figure 9. Global analysis of fluorescence upconversion decays of P3HT in MCH at 20 °C, measured with λ_{exc} = 420 nm at the onset and tail of the emission band (540 and 630 nm) and 50 fs steps. τ, A, reduced χ^2 values, weighted residuals, and ACs are shown. The instrumental response signal is shown in blue. The long-lived growing at 630 nm is clearly seen.

found as expected for nonexponential decays resulting from energy transfer measured with better time resolution. The 20 and 500 ps (too long to be defined in the observed time window, ca. 20 ps) were fixed in the analysis. Basically, the decays continue to consist of the polymer lifetime (500 ps) plus a decay (at the onset) or rise (at the tail) function that, within this time range, can be fitted with a sum of three exponential terms. It is worth remembering that, because the theoretical decay of energy transfer is not a discrete sum of exponential terms, each decay time and preexponential coefficient obtained from multiexponential fittings is a fitting parameter, dependent on the covering detail (resolution) of the inspected time range. On the other hand, the fluorescence decays of the trimer (T3HT) instead of showing this complex function, just show a 200 fs plus a very minor 3 ps decay besides the trimer lifetime (142 ps from single-exponential ps-TCSPC decays). Moreover, this value is identical to the trimer (α-therthienyl), 150 ps,[36] with no alkyl chains thus showing that in the large majority of the oligo- and polythiophenes conformational relaxation plays a minor role in the deactivation of the singlet excited state. Because energy transfer is absent in the trimer, the fast part of the T3HT decays should be assigned to solvent relaxation. The 3 ps component is close to the 5 ps component observed in the Stokes-shift correlation function of the 2,5-bis[(3′-methylbutyl)oxy]-p-phenylenevinylene trimer in MCH at 20 °C, in addition with the 20 ps torsional relaxation time.[37] A detailed investigation of the photophysics of the T3HT and of D3HT (dimer) will be published elsewhere.

Summarizing at this stage, the isolated chains of HT-RR-P3HT do not show experimentally detectable conformational relaxation and the two shortest exponential terms of the fluorescence decays essentially result from intrachain energy transfer.

Low-Temperature Excited-State Dynamics (Aggregates and Film). Below −10 °C, the polymer forms ground-state dimer-like aggregates, showing vibrational structured absorption and emission bands similar to those observed in films. The vibrational structure is attributed to a deep minimum in the ground-state energy surface of the dimer or aggregate. Consequently, the fluorescence decays become more complex due to the contributions of both isolated and aggregated polymer chains. The separation of these would

require excitation wavelengths above 550 nm, which are not currently available with our ps-TCSPC equipment. However, below −40 °C the fluorescence at 670 nm is essentially due to direct excitation of aggregates as seen in Figure 1. Therefore, these decays were analyzed individually, and the results are shown in Table 2.

Table 2. Decay Times and Preexponential Coefficients Recovered from Individual Analysis of the Fluorescence Decays of P3HT in MCH Measured at λ_{em} = 670 nm, from −40 to −70 °C

T (°C)	τ_3 (ps)	τ_2 (ps)	τ_1 (ps)	A_3	A_2	A_1
−40	132	580	1360	0.27	0.40	0.33
−50	153	713	1590	0.30	0.41	0.28
−60	151	613	1500	0.33	0.36	0.32
−70	128	563	1500	0.37	0.37	0.26

The fluorescence decays of the aggregates are reasonably fit with sums of three exponentials, as expected from the small values of $A_{4,670}$ below −40 °C. The preexponential coefficients indicate that ca. 90% of the aggregates fluorescence is due to the two longer lived components: the 500 ps component (here ca. 600 ps), characteristic of isolated chains, and the 1.5 ns component, characteristic of aggregates. The similarity of the preexponential coefficients A_1 and A_2 indicate approximately equal fractions of chains or chain segments in "isolated-chain" and "dimer-like" conformations in equilibrium.

The relatively long decay times with large preexponential coefficients are consistent with an average fluorescence quantum yield for the aggregates not much different from that obtained for isolated polymer chains (ϕ_F = 0.20 for RR-P3HT polymers with M_w = 60 kDa in toluene (work in progress), and ϕ_F = 0.33 for M_w = 55 kDa[20]). In fact, although the fluorescence quantum yield of the aggregates has not been measured in this work, parts a and b of Figure 1 show that the fluorescence of the aggregates are ca. 5-fold lower than that of isolated chains with excitation at 440 nm where the molar excitation wavelength of the aggregate is ca. 3-fold lower than that of the isolated chain; i.e., ϕ_F(aggregate) ≈ 3/5 ϕ_F(isolated chain). The relatively high quantum yield and mean lifetime of the aggregates indicates that the expected increase in the internal conversion rate constant from an isolated chain to the dimer-like aggregate (smaller S_1–S_0 energy gap) is not substantial.

Because the spectral similarities between film and aggregates indicate similar electronic first singlet excited states (and oscillator strengths), the huge decrease in the fluorescence quantum yield and average decay time from aggregates to film [ϕ_F (film) = 0.02[20]] indicates the presence in the film of additional processes that are able to efficiently compete with the radiative decay. Taking into consideration that internal conversion (phonon emission) is not expected to dramatically increase (more than an order of magnitude for P3HT) from solution to film and that triplet-state formation has not been observed for regio-regular P3HT films,[20,38,39] we propose that the strong fluorescence quenching of P3HT in films may result from efficient (ultrafast) interchain exciton dissociation with eventual contribution of singlet–singlet annihilation (only significant for singlet densities above ~1 × 10^{12} incident photons/cm^2, i.e., for the ps-FUC measurements).[40] The fact that in P3HT films the exciton involves molecular orbitals belonging to at least two polymer chains (two-dimensional

interchain character)[41] could be the cause for a low exciton binding energy, which is implicit in our hypothesis of fast exciton dissociation. Alternatively, the microcrystalline domains formed by the dimer-like aggregates in P3HT[41] could provide phonon modes capable of substantially increasing internal conversion, which could be then the cause for the strong fluorescence quenching in film (fast exciton decay to the ground state). Fast transient absorption spectroscopy (femtosecond pump−probe) data coupled to the foregoing data likely would provide the basis for a decision whether both or which of the two alternatives is correct. This will be considered in forthcoming work. In conclusion, the comparison of the primary processes occurring in film with those that occur in aggregates seems promising toward a better clarification of the rather complex photophysics of P3HT in film.

Aging of Films. The effect of film aging on the contribution of the 500 ps component seems to indicate film degradation, although differences in film preparation such as annealing vs nonannealing are known to induce important changes on the photophysical properties of P3HT films.[42] In our case, however, degradation in the absence of oxygen and/or water (films were kept in the glovebox) does not seem much plausible. Because the 500 ps component is the fingerprint of isolated P3HT chains, which may be seen as a film "defect", an alternative explanation would be that, due to the relatively low glass transition temperature of polythiophenes,[43] slow (in 2 months) rearrangement of chains to form the more stable aggregate-like conformation could take place at room temperature, thus lowering the 500 ps contribution in the fluorescence decay of the film. This possibility is presently under study.

CONCLUSIONS

From the foregoing results and discussion, essentially two conclusions may be derived. First, HT-RR-P3HT isolated chains do not show torsional relaxation in the picosecond time domain. The earlier events after photoexcitation are assigned to intrachain energy transfer from high to lower energy excitons. Second, HT-RR-P3HT in aggregates shows absorption and fluorescence spectra similar to HT-RR-P3HT films but much larger fluorescence quantum yield and longer decay times. The strong quenching of the fluorescence in film vs aggregate is thus assigned to fast interchain exciton and/or phonon induced internal conversion, followed by slower processes not leading to radiative dissociation exciton recombination from the singlet excited state.

AUTHOR INFORMATION

Corresponding Author
*E-mail: palmira@ist.utl.pt (P.F.d.S.); macanita@ist.utl.pt.

Notes
The authors declare no competing financial interest.

ACKNOWLEDGMENTS

REFERENCES

(1) Pina, J.; Burrows, H. D.; Seixas de Melo, J. S., Excited state dynamics in pi-conjugated polymers. In *Specialist Periodic Reports in Photochemistry*; Albini, A., Ed. Royal Society of Chemistry: Cambridge, U.K., 2011; Vol. 39, p 30.

(2) Hwang, I. W.; Moses, D.; Heeger, A. J. *J. Phys. Chem. C* **2008**, *112*, 4350.

(3) Trotzky, S.; Hoyer, T.; Tuszynski, W.; Lienau, C.; Parisi, J. *J. Phys. D: App. Phys.* **2009**, *42*, 055105.

(4) Nelson, J.; Choulis, S. A.; Durrant, J. R. *Thin Solid Films* **2004**, *451*, 508.

(5) Piris, J.; Dykstra, T. E.; Bakulin, A. A.; van Loosdrecht, P. H. M.; Knulst, W.; Trinh, M. T.; Schins, J. M.; Siebbeles, L. D. A. *J. Phys. Chem. C* **2009**, *113*, 14500.

(6) Xie, Y.; Li, Y.; Xiao, L. X.; Qiao, Q. Q.; Dhakal, R.; Zhang, Z. L.; Gong, Q. H.; Galipeau, D.; Yan, X. Z. *J. Phys. Chem. C* **2010**, *114*, 14590.

(7) Schilinsky, P.; Asawapirom, U.; Scherf, U.; Biele, M.; Brabec, C. J. *Chem. Mater.* **2005**, *17*, 2175.

(8) Dogariu, A.; Vacar, D.; Heeger, A. J. *Phys. Rev. B* **1998**, *58*, 10218.

(9) Dias, F. B.; Maçanita, A. L.; Seixas de Melo, J.; Burrows, H. D.; Guntner, R.; Scherf, U.; Monkman, A. P. *J. Chem. Phys.* **2003**, *118*, 7119.

(10) Pina, J.; Seixas de Melo, J.; Burrows, H. D.; Maçanita, A. L.; Galbrecht, F.; Bunnagel, T.; Scherf, U. *Macromolecules* **2009**, *42*, 1710.

(11) Pina, J.; Seixas de Melo, J.; Burrows, H. D.; Bunnagel, T. W.; Dolfen, D.; Kudla, C. J.; Scherf, U. *J. Phys. Chem. B* **2009**, *113*, 15928.

(12) Di Paolo, R. E.; Seixas de Melo, J.; Pina, J.; Burrows, H. D.; Morgado, J.; Maçanita, A. L. *ChemPhysChem* **2007**, *8*, 2657.

(13) Scholes, G. D. *Annu. Rev. Phys. Chem.* **2003**, *54*, 57.

(14) Heun, S.; Mahrt, R. F.; Greiner, A.; Lemmer, U.; Bassler, H.; Halliday, D. A.; Bradley, D. D. C.; Burn, P. L.; Holmes, A. B. *J. Phys.: Condes. Matter* **1993**, *5*, 247.

(15) Meskers, S. C. J.; Hubner, J.; Oestreich, M.; Bassler, H. *J. Phys. Chem. B* **2001**, *105*, 9139.

(16) Bredas, J. L.; Beljonne, D.; Coropceanu, V.; Cornil, J. *Chem. Rev.* **2004**, *104*, 4971.

(17) Xie, Y.; Li, Y.; Xiao, L. X.; Qiao, Q. Q.; Dhakal, R.; Zhang, Z. L.; Gong, Q. H.; Galipeau, D.; Yan, X. Z. *J. Phys. Chem. C* **2010**, *114*, 14590.

(18) Parkinson, P.; Muller, C.; Stingelin, N.; Johnston, M. B.; Herz, L. M. *J. Phys. Chem. Lett.* **2010**, *1*, 2788.

(19) Westenhoff, S.; Beenken, W. J. D.; Friend, R. H.; Greenham, N. C.; Yartsev, A.; Sundstrom, V. *Phys. Rev. Lett.* **2006**, *97*, 166804.

(20) Cook, S.; Furube, A.; Katoh, R. *Energy Environ. Sci.* **2008**, *1*, 294.

(21) Shaw, P. E.; Ruseckas, A.; Samuel, I. D. W. *Adv. Mater.* **2008**, *20*, 3516.

(22) Banerji, N.; Cowan, S.; Vauthey, E.; Heeger, A. J. *J. Phys. Chem. C* **2011**, *115*, 9726.

(23) Rodrigues, R. F.; da Silva, P. F.; Shimizu, K.; Freitas, A. A.; Kovalenko, S. A.; Ernsting, N. P.; Quina, F. H.; Maçanita, A. *Chem.—Eur. J.* **2009**, *15*, 1397.

(24) Striker, G.; Subramaniam, V.; Seidel, C. A. M.; Volkmer, A. *J. Phys. Chem. B* **1999**, *103*, 8612.

(25) Liu, J. G.; Sun, Y.; Gao, X. A.; Xing, R. B.; Zheng, L. D.; Wu, S. P.; Geng, Y. H.; Han, Y. C. *Langmuir* **2011**, *27*, 4212.

(26) Yamamoto, T.; Komarudin, D.; Arai, M.; Lee, B.-L.; Suganuma, H.; Asakawa, N.; Inoue, Y.; Kubota, K.; Sasaki, S.; Fukuda, T.; Matsuda, H. *J. Am. Chem. Soc.* **1998**, *120*, 2047.

(27) Wells, N. P.; Boudouris, B. W.; Hillmyer, M. A.; Blank, D. A. *J. Phys. Chem. A* **2007**, *111*, 15404.

(28) Westenhoff, S.; Beenken, W. J. D.; Friend, R. H.; Greenham, N. C.; Yartsev, A.; Sundstrom, V. *Phys. Rev. Lett.* **2006**, *97*, 166804.

(29) Peng, Q. L.; Wyman, I. W.; Han, D. H.; Liu, G. J. *Can. J. Chem. (Rev. Can. Chim.)* **2011**, *89*, 27.

(30) McNeill, C. R.; Abrusci, A.; Hwang, I.; Ruderer, M. A.; Muller-Buschbaum, P.; Greenham, N. C. *Adv. Funct. Mater.* **2009**, *19*, 3103.

(31) Collison, C. J.; Rothberg, L. J.; Treemaneekarn, V.; Li, Y. *Macromolecules* **2001**, *34*, 2346.

(32) Markov, D. E.; Blom, P. W. M. *Appl. Phys. Lett.* **2005**, *87*, 233511.

(33) Scheblykin, I. G.; Yartsev, A.; Pullerits, T.; Gulbinas, V.; Sundstrom, V. *J. Phys. Chem. B* **2007**, *111*, 6303.

(34) Maroncelli, M.; Fleming, G. R. *J. Chem. Phys.* **1987**, *86*, 6221.

(35) Yekta, A.; Winnik, M. A.; Farinha, J. P. S; Martinho, J. M. G. *J. Phys. Chem. A* **1997**, *101*, 1787.

(36) Becker, R. S.; Seixas de Melo, J.; Maçanita, A. L.; Elisei, F. *J. Phys. Chem.* **1996**, *100*, 18683.

(37) Di Paolo, R. E.; Gigante, B.; Esteves, M. A.; Pires, N.; Santos, C.; Lameiro, M. H.; Seixas de Melo, J.; Burrows, H. D.; Maçanita, A. L. *ChemPhysChem* **2008**, *9*, 2214.

(38) Osterbacka, R.; An, C. P.; Jiang, X. M.; Vardeny, Z. V. *Science* **2000**, *287*, 839.

(39) Ohkita, H.; Cook, S.; Astuti, Y.; Duffy, W.; Tierney, S.; Zhang, W.; Heeney, M.; McCulloch, I.; Nelson, J.; Bradley, D. D. C.; Durrant, J. R. *J. Am. Chem. Soc.* **2008**, *130*, 3030.

(40) Cook, S.; Han, L. Y.; Furube, A.; Katoh, R. *J. Phys. Chem. C* **2010**, *114*, 10962.

(41) Sirringhaus, H.; Brown, P. J.; Friend, R. H.; Nielsen, M. M.; Bechgaard, K.; Langeveld-Voss, B. M. W.; Spiering, A. J. H.; Janssen, R. A. J.; Meijer, E. W.; Herwig, P.; de Leeuw, D. M. *Nature* **1999**, *401*, 685.

(42) Kanai, K.; Miyazaki, T.; Suzuki, H.; Inaba, M.; Ouchi, Y.; Seki, K. *Phys. Chem. Chem. Phys.* **2010**, *12*, 273.

(43) Zhao, J.; Swinnen, A.; Van Assche, G.; Manca, J.; Vanderzande, D.; Van Mele, B. *J. Phys. Chem. B* **2009**, *113*, 1587.